Precision Agric (2018) 19:823–839
https://doi.org/10.1007/s11119-018-9559-4

Nutrient quantification in fresh and dried mixtures of ryegrass and clover leaves using laser-induced breakdown spectroscopy

H. Jull[1] · **R. Künnemeyer**[1] · **P. Schaare**[2]

Published online: 25 January 2018

Abstract Laser-induced breakdown spectroscopy (LIBS) is an analytical technique that can be used to facilitate variable rate fertilizer application, potentially increasing yield, reducing costs and reducing environmental side effects of nutrient loss. LIBS can give real-time information about macro and micro nutrients with little to no sample preparation. The study reported in this paper investigated whether LIBS can predict nutrient levels of fresh and dried pelletized pasture and what the limitations are. Spectra were acquired in air and under argon. Partial least square regression was used to build models for each macro and micro nutrient. The best results were for potassium, sodium and manganese with root mean square errors of cross-validation of 0.20, 0.029 and 0.0008 wt%, respectively, coefficient of determination of 0.92, 0.93 and 0.90, limits of detection of 0.99, 0.11 and 0.0027 wt%, and precisions of 0.30, 0.042 and 0.0012 wt%. LIBS can be used to assess nutrient levels of fresh pasture. Reducing the shot-to-shot variation will lead to improved calibrations.

Keywords Laser-induced breakdown spectroscopy · Pasture · Partial-least squares regression · Plant Nutrition

Introduction

Insufficient fertilizer deprives soil and crops of much needed nutrients, while too much fertilizer increases cost and pollution in streams and rivers. Knowing what nutrients are needed and where to apply them may overcome these problems. Precision agriculture is creating financial and environmental benefits through site-specific and precisely timed crop management. This is achieved through technologies guiding variable rate applications of

✉ H. Jull
harrisson.jull@gmail.com

[1] School of Engineering, The Dodd Walls Centre for Photonic and Quantum Technologies, The University of Waikato, Hamilton 3240, New Zealand

[2] Plant and Food Research, Hamilton 3240, New Zealand

fertilizer (van Maarschalkerweerd and Husted 2015). Essential elements required for plant growth are classified according to the quantities required as either macro or micro nutrients (Barker and Pilbeam 2006). Generally macro nutrients [nitrogen (N), phosphorus (P), potassium (K), calcium (Ca), sulfur (S) and magnesium (Mg)] are larger than 0.1 wt% and micro nutrients [boron (B), chlorine (Cl), manganese (Mn), iron (Fe), zinc (Zn), copper (Cu), molybdenum (Mo) and nickel (Ni)] are less than 0.01 wt%. Na is not an essential nutrient but can be beneficial in stimulating growth (Gorham 2006). Precision agriculture is based on measurements which must be rapid and cost-effective so sufficient data can be acquired for spatial and temporal precision. The measurements must be selective to avoid interference and unstable calibration and they need to be sensitive if measuring low concentrations. Laser induced breakdown spectroscopy (LIBS) is a method that could potentially satisfy these requirements.

LIBS has become a very popular analytical method in the last decade, due to unique features such as applicability to any type of sample, practically no sample preparation, remote sensing capability and speed of analysis. Analysis of leaf nutrient content is a complex laboratory-based process involving wet chemistry and powerful chemicals for digesting plant fiber; it typically costs tens of dollars per sample and requires considerable time. Consequently, when evaluating nutrient requirements, leaf material is sampled at course spatial resolution, reducing potential benefits of variable rate application. LIBS can eliminate these constraints.

LIBS is a type of optical emission spectroscopy where a high powered pulsed laser, usually a Q-switched laser, is focused onto the surface of a material. The high power density breaks down the surface material and creates a plasma once the breakdown threshold is exceeded (Cremers and Radziemski 2013a). The breakdown threshold depends on the surface material of the sample. When the plasma is created, the remaining part of the laser pulse is absorbed causing the plasma temperature to increase (Cremers and Radziemski 2013b). As the plasma cools, electrons transition from high to low energy levels. Each element has specific energy levels where transitions can take place resulting in emission of photons of distinct wavelength. The intensities of these emissions are related to the concentrations of the elements observable in the recorded spectrum (Thakur 2007).

A major problem when creating calibration models for LIBS is the lack of repeatability (Hahn and Omenetto 2012). The variations between spectra from the same sample, and between samples, are caused by many factors including inhomogeneity, matrix effects and perturbations in experimental parameters. Sample moisture is another factor that changes the intensities between identical samples. The moisture in a sample has been found to reduce the intensity of emission lines and the limits of detection (Lazic et al. 2007; Rauschenbach et al. 2008). Reduction of moisture in a sample reduces the power density required to produce breakdown in the sample. This increases the amount of ablated sample, temperature in the plasma and the intensity of the emission. The temperature dependence of plasmas, caused by the exponential Boltzmann factor and the partition function within the emission line intensity equation, is one of the leading factors contributing to variability between spectra from the same sample. There are various techniques to reduce the adverse effects these factors have on a calibration curve including averaging multiple spectra from the same sample, using internal standards and using chemometric techniques. Argon atmospheres have also been used to increase the temperature in the plasma which increases the intensity of the spectral lines and also increases the number of emission lines observed. This creates more lines to analyze with higher signal to noise ratio which increases the predictive capability of LIBS. Temperature correction and internal standardization, to improve the prediction of the calibration curves on pelletized pasture, was investigated in a

previous paper (Jull et al. 2015). Considerations of emission line selection for normalizations specifically for pasture were discussed. Some of these considerations include emission lines having similar ionization energies, excitation energies and intensities (Barnett et al. 1968).

Few studies have been done using LIBS on pasture and, to the authors' knowledge, none on fresh pasture. LIBS, on pelletized samples, was used by Martin et al. (2010) to determine whether endophyte infection in Tall Fescue Grass (*Festuca arundinacea*) could be identified. Differentiation between healthy and infected samples was unsuccessful due to the lack of samples. Calcium, magnesium, iron, manganese, zinc, lead and cadmium were detected in the grass samples. The efficiency of multivariate and univariate calibrations on micro nutrients in pelletized plant materials was studied by Braga et al. (2010). Grass (*Axonopus obtusifolius*) was used to validate their calibration models. To reduce shot-to-shot variations and matrix effects, all emission lines were normalized by the C I 193.09 nm emission line. The expected values could be predicted by the multivariate model but not by the univariate model. The authors concluded that the chemical and physical makeup of the material used for calibration should be similar to the plant species to be studied if a reduction in matrix effects was to be observed.

Bermuda grass (*Cynodon dactylon*) and Plantain stems (*Musa paradisiaca*) were examined by Rai et al. (2009) to find which elements are responsible for their glycemic attributes. Powdered extracts were dissolved in distilled water and multiple LIBS spectra were recorded. Emission lines for both samples were normalized with the C III 229.7 nm line and compared. The Mg, K and Na concentrations were responsible for the antidiabetic effects of Bermuda grass. The distribution of silicon in Bermuda grass was studied by Chauhan et al. (2011). Phytolith analysis was used to determine the concentration of silicon in the grass samples. The spectra showed that the highest concentration of Si is found in the leaf blade, followed by the leaf sheath and stem.

Spectra from grass fragments and pollen were compared by Boyain-Goitia et al. (2003) in their work on bio-aerosols. A reduction in matrix effects was achieved by normalizing the spectra by the CN violet bands. Chromium and iron lines were observed only in the spectra from pollen. Calcium and aluminum were similar in both samples. Silicon emissions were found in spectra from grass which was likely caused by soil dust on the samples. A lack of samples was responsible for the struggle differentiating between pollen and grass fragments. Devey et al. (2015) compared LIBS results for pelletized pasture samples with inductively coupled plasma-optical emission spectroscopy (ICP-OES). Savitzky–Golay smoothing followed by vector normalization and wavelet smoothing was performed before partial least-squares regression (PLS) models were created on selected spectral regions. Sodium, potassium, calcium and phosphorus had accuracies similar to the ICP-OES results. Manganese, iron and boron had reasonable results but zinc, copper and sulphur did not.

The work presented in this paper investigates, for the first time, the viability of using LIBS in-field to measure micro and macro nutrients in fresh untreated pasture. Measurements were made on fresh and dried, pelletized pasture both in air and under an argon atmosphere. Precision, limits of detection and root-mean square error of cross-validation were used to compare prediction models.

Materials and methods

A commercial LIBS system (LIBS-6, Applied Photonics, Skipton, UK) system with a Nd:YAG laser (Big Sky Ultra, Quantel, France) operating at 1064 nm with a pulse width of 7 ns, and pulse energy of 100 mJ was focused perpendicular to the sample surface to generate the plasma. The setup had a fixed distance to the sample. The LIBS-6 has a built-in beam expander which was focused to roughly 80 mm from the beam expander. The surfaces of the samples were placed 79 mm from the beam expander which corresponded to the lens-to-sample distance that produced the highest emission line intensities. The spot size on the sample was 450 μm, measured from the crater, which produced an irradiance of 9.0 GW cm^{-2}. Each spectrum was acquired with the six (Avantes, Apeldoorn, The Netherlands) spectrometers in the LIBS-6 unit covering the range 182.26–908.07 nm. All spectrometers were set to start recording after a delay time of 1.27 μs with respect to the laser pulse and an integration time of 1 ms. A 3-axis translation stage was employed so that each sample surface was at the same height. The translation stage moved the sample so that each LIBS pulse was aimed at a new location.

Fresh pasture (a mix of ryegrass and clover leaves), from 20 different plots of typical grazing paddocks in the Waikato region of New Zealand, was harvested over a 13 month period creating a total of 280 samples. The herbage was pressed flat in a holder. An accumulation of 100 shots under an air atmosphere, and 100 shots under an argon purge were taken for each batch. Each shot was taken from a new location on the sample. The pasture samples were sent to a commercial analytical laboratory where they were dried at 62 °C overnight and ground to pass through a 1 mm screen. Nitrogen was estimated by NIR calibration based on N by Dumas combustion. All other elements were determined by nitric acid/hydrogen peroxide digestion followed by inductively coupled plasma optical emission spectrometry. Table 1 shows the variation in the dataset and the limits of detection for the quantitative analysis performed by the laboratory. A portion of the powder was returned and pellets were pressed for each batch of harvested pasture. An accumulation of 100 shots under an air atmosphere, and 100 shots under an argon purge were taken for each pellet. Each shot was taken from a new location on the sample.

Partial least squares regression (PLS) is a statistical technique that has been employed to overcome the drawbacks of variability between spectra. PLS is a technique that is used

Table 1 Concentration range (wt%) of the data set and detection limits of the commercial analytical laboratory

Element	Mean	SD	Detection limit of reference
N	2.8	0.49	0.1
P	0.36	0.054	0.02
K	2.7	0.68	0.1
S	0.33	0.042	0.02
Ca	0.68	0.18	0.02
Mg	0.19	0.03	0.02
Na	0.26	0.12	0.002
Fe	0.01	0.0082	0.0005
Mn	0.0061	0.0025	0.0003
Zn	0.0044	0.0057	0.0002
Cu	0.00075	0.00018	0.0001
B	0.00062	0.0003	0.0001

when there are many variables, compared to observations, and when there is high collinearity, in the data, between variables. This is well suited to LIBS spectra that have thousands of variables, many of which are collinear. By projecting the elemental concentrations (responses) and the spectra (predictors) to a new space, PLS finds a fundamental linear relationship between the predictors and responses. An underlying relationship can be found that is not necessarily visually apparent. This relationship is conveyed through the Latent Variables (LV). PLS has found great success building calibration curves that perform better than simple linear regression of a single emission line (Fink et al. 2002; Nunes et al. 2010). There are various methods of determining which variables are important in a PLS model (Mehmood et al. 2011). Variable Importance on Projections (VIP) scores on the predictors is an indication of the significance of the projections to find the latent variables. VIPs are calculated as (Wold et al. 1993):

$$\mathrm{VIP_j} = \sqrt{p \sum_{m=1}^{M} w_{mj}^2 SS(b_m t_m) / \left(\sum_{m=1}^{M} SS(b_m t_m) \right)} \tag{1}$$

where p is the number of variables in a predictor, M is the number of LVs, $SS(b_m t_m)$ is the percentage of y explained in the mth latent variable and w_{mj} is the weight for the jth variable for the mth latent variable. A cut-off criterion for variable selection of VIP scores greater than one is usually used, since the average value of all VIP scores equals one. Performing VIP after PLS has produced excellent results in detecting relevant predictors and has outperformed other variable selection methods (Chong and Jun 2005).

The accuracy of a PLS model is measured by the difference between the predicted values and actual values. The Root Mean Squared Error of Cross-Validation (RMSECV) parameter is one measure of these differences. The RMSECV is calculated as:

$$\mathrm{RMSECV} = \sqrt{\frac{\sum_{i=1}^{n} (\hat{y}_i - y_i)^2}{n}} \tag{2}$$

where $\hat{y}$ contains the predictions from the cross-validation for the ith samples which was not used in building the model for that fold, y contains the actual responses and n is the number of samples.

There are various figures of merit used to assess the performance of an analysis method. These include precision and limits of detection. Precision is used as a metric for measurement repeatability. This is usually represented in the standard deviation of a group of measurements on the same sample. Precision is calculated as (ASTM E1655-05 2012):

$$\mathrm{s} = \sqrt{\frac{\sum_{i=1}^{n} \sum_{j=1}^{m} \left(\hat{\bar{y}}_i - \hat{y}_{i,j} \right)^2}{n(m-1)}} \tag{3}$$

where $\hat{\bar{y}}$ is the mean of the predictions for the replicates in a sample, $\hat{y}$ are the predictions for a sample, n is the number of samples and m is the number of replicates. In this study, n and m are five and ten respectively and each replicate is the average of ten measurements.

The limit of detection (LOD) is the smallest concentration that can be detected with reasonable certainty (Boqué and Rius 1996). For PLS this value can be calculated as (Allegrini and Olivieri 2014; Ortiz et al. 2003):

$$\mathrm{LOD} = 3.3 s_{pu}^{-1} \left[\left(1 + \frac{\bar{y}_{cal}^2}{\sum_{i=1}^{I} y_i^2} + 1/I \right) var_{pu} \right]^{1/2} \quad (4)$$

where s_{pu} is the slope of the calibration line, var_{pu} is the variance of the regression residuals, $\bar{y}_{cal}^2$ is the mean calibration concentration, I is the number of samples, and y_i is the centered concentration.

All spectra were corrected for background and dark current. Three samples were removed because of false laboratory results. The 100 spectra for each sample were averaged but not normalized. The resulting spectra were then analyzed using PLS with 10-fold cross-validation in Matlab (R2012a, MathWorks, Natick, USA). Matlab uses the SIMPLS algorithm which centers both the predictors and responses. Calibration models were generated for N, P, K, S, Ca, Mg, Na, Fe, Mn, Zn, Cu and B.

Results and discussion

A typical LIBS spectrum for fresh and pelletized pasture is shown in Fig. 1. The strongest emission lines for each element are listed in Table 2. The spectra display increased intensities for samples under argon and an intensity reduction for the oxygen triplet around 777 nm. This is expected as argon has a low ionization energy which contributes more electrons into the plasma, and the presence of argon reduces the surrounding oxygen concentration.

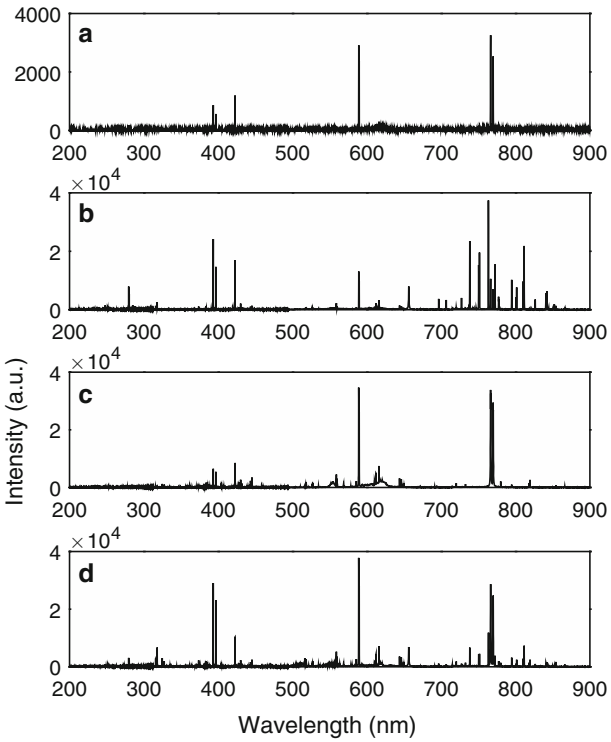

Fig. 1 Typical spectra for fresh pasture in air (**a**), fresh pasture under argon (**b**), pelletized pasture in air (**c**), and pelletizedpasture under argon (**d**)

Table 2 Strong emission lines of nutrients in pasture

Species	Strong emission lines (nm)
N I	742.36, 744.23, 746.83, 862.92, 868.03, 868.34
P I	167.97, 177.50
K I	691.11, 693.88, 766.49, 769.90
S I	142.50, 147.40, 180.73
Ca I	422.67, 442.54, 443.50, 445.48
Ca II	315.89, 317.93, 393.37, 396.85
Mg I	285.21, 382.94, 383.23, 383.82, 516.73, 517.27, 518.36
Na I	589.00, 589.59, 818.33, 819.48
Fe I	358.12, 371.99, 373.71, 374.56, 374.59, 374.83
Fe II	238.20, 239.56, 240.49, 241.05, 241.33
Mn I	403.08, 403.31, 403.45
Zn I	213.86, 334.50, 481.05
Cu I	324.75, 327.40, 521.82
B I	249.68, 249.77

Multiple PLS models were built for each element by repeatedly performing 10-fold cross-validation on the spectra then increasing the number of LVs. The RMSECVs were observed and the number of optimal LVs were chosen corresponding to lowest RMSECVs. Table 3, Figs. 2 and 3 display the PLS prediction results from the 10-fold cross-validations for the elemental concentrations in the samples. Precision was calculated from the pooled values in each fold of the cross-validation. The calculated RMSECV for the dried pellets were similar to the results obtained by Devey et al. (2015).

The use of argon on fresh pasture produced models with greater coefficient of determination (R^2) for all elements except P (R^2 results for fresh samples under argon are not shown). It produced inferior precision for all elements and reduced the RMSECV in all elements except P, Ca and Cu. It also improved LOD for Ca with slight increases for S, Mg, Na, Fe, Mn and Zn. Using argon on pelletized pasture reduced the RMSECV for all elements and enhanced the R^2 for all elements except S, Ca, Mn and B (R^2 results for pellet samples in air are not shown). The LOD improved for N, P, Mg, Na, Fe, Zn and Cu. Precision for N, K, Ca, Mg, Fe, Zn and Cu were also improved. When comparing fresh and dried pasture, there was a reduction in RMSECV for all elements in dried pasture and an increase in R^2 for all elements. Fresh pasture had better precision for N, P, S, Fe, Zn and Cu, but worse LOD for all elements. The best correlations were found for K and Na in pellets sampled under argon and Mg in pellets sampled in air. The values of R^2 were 0.92, 0.93 and 0.90 respectively. K and Mg were the only elements to have R^2 over 0.7 for fresh pasture in air.

Dried pellets had better RMSECV and R^2 results because there is less between-sample variation caused by the different moisture levels between each fresh sample. During March 2014, the middle of the 13 month period, there was a drought in New Zealand. K, Mg and Fe concentrations were affected by this. Mg and Fe levels were significantly higher and K levels were significantly lower. This provided a wider range of concentrations to build models on and accounts for the two groupings seen in some of the calibration curves for some elements.

Table 3 Accuracy of PLS models created for the macro and micro nutrients in pasture

	Element	In air				Under argon			
		LV	Precision	RMSECV	LOD	LV	Precision	RMSECV	LOD
Fresh	N	6	0.31	0.4	1.7	7	0.79	0.36	2.5
Pasture	P	10	0.026	0.043	0.16	6	0.088	0.044	0.3
	K	24	0.45	0.35	1.2	12	0.63	0.33	1.6
	S	7	0.029	0.037	0.15	31	0.07	0.035	0.13
	Ca	3	0.16	0.14	0.82	10	0.25	0.14	0.56
	Mg	18	0.025	0.021	0.078	16	0.037	0.02	0.075
	Na	6	0.056	0.084	0.29	35	0.11	0.08	0.27
	Fe	21	0.0039	0.0051	0.017	35	0.0068	0.0041	0.014
	Mn	21	0.0012	0.0013	0.0044	23	0.0021	0.001	0.0036
	Zn	26	0.00084	0.0009	0.0029	14	0.001	0.0008	0.0026
	Cu	23	0.00011	0.00011	0.00039	15	0.00021	0.00011	0.00039
	B	6	0.000097	0.00025	0.00087	10	0.00032	0.00024	0.00086
Pellets	N	14	0.44	0.31	1.3	43	0.39	0.26	0.97
	P	27	0.044	0.032	0.12	48	0.05	0.032	0.11
	K	19	0.42	0.22	0.93	12	0.3	0.2	0.99
	S	44	0.041	0.029	0.11	46	0.046	0.032	0.12
	Ca	41	0.15	0.066	0.22	18	0.13	0.08	0.31
	Mg	27	0.022	0.013	0.05	48	0.021	0.013	0.047
	Na	15	0.04	0.03	0.12	18	0.042	0.029	0.11
	Fe	42	0.0044	0.0033	0.011	50	0.004	0.0029	0.0096
	Mn	38	0.0012	0.00075	0.0025	37	0.0012	0.0008	0.0027
	Zn	38	0.00089	0.00069	0.0026	39	0.00081	0.00058	0.002
	Cu	31	0.00015	0.000095	0.00034	46	0.0001	0.000089	0.00031
	B	34	0.000097	0.00025	0.00042	45	0.00032	0.00024	0.00049

Concentrations are in wt%

Nitrogen

The nitrogen emission lines are very weak in the collected spectra. One reason is that the upper level energies of the strong nitrogen emission lines are about 12.0 eV. The plasmas created in this study do not have sufficient energy to allow sufficient population of these states. Another reason is the contribution of nitrogen from the atmosphere. The atmospheric nitrogen would add to, or even overwhelm, the nitrogen concentration in the samples when measured in air. Under an argon atmosphere, the effect of atmospheric nitrogen is reduced, improving results. Figure 4 displays the intensity of the strongest nitrogen line (N I 746.83 nm) for fresh pasture in air which had a VIP score of 18. The emission line intensities were larger even though the nitrogen concentrations were lower. These larger intensities are from samples collected March 2014 when there was a drought in New Zealand. The high intensities are likely caused by a reduction of moisture in the sample. Nitrogen line intensities appeared more consistent outside the drought period. The highest VIP scores for fresh pasture in air were 1777, 1016, 642 and 491 for K I

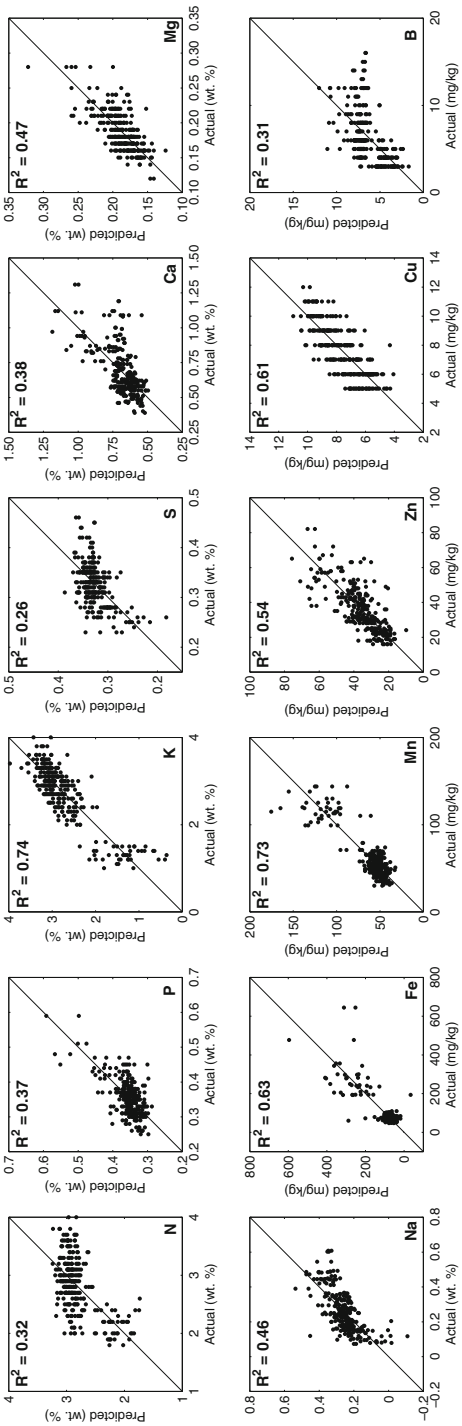

Fig. 2 Predictions created from PLS 10-fold cross-validation on fresh pasture in air

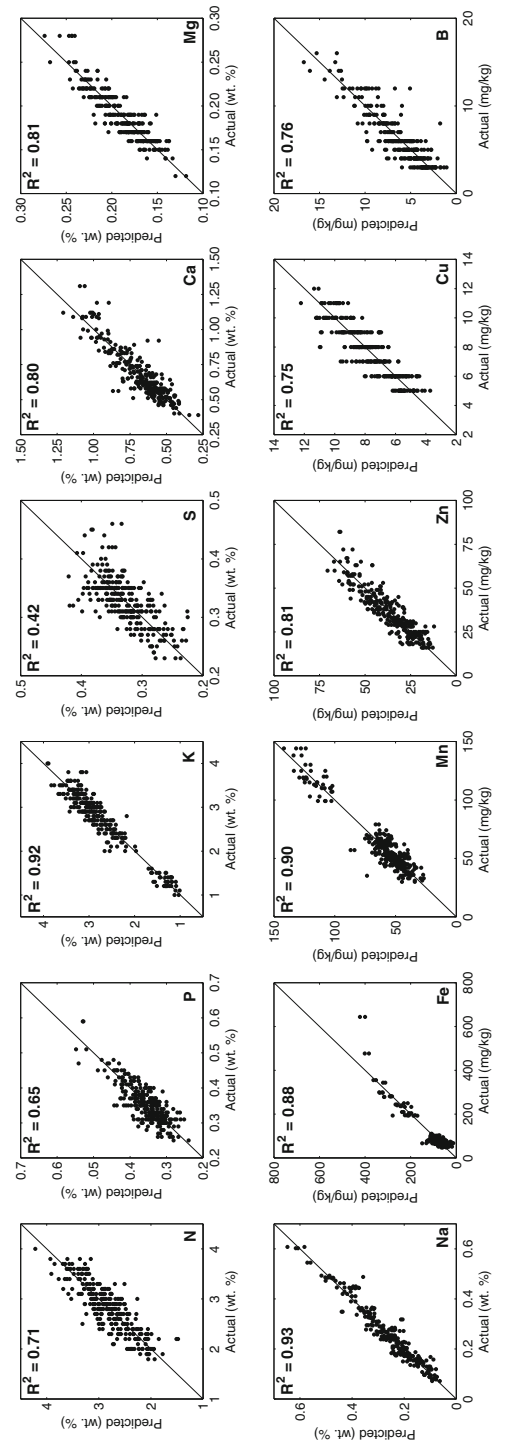

Fig. 3 Predictions created from PLS 10-fold cross-validation on pelletized pasture under argon

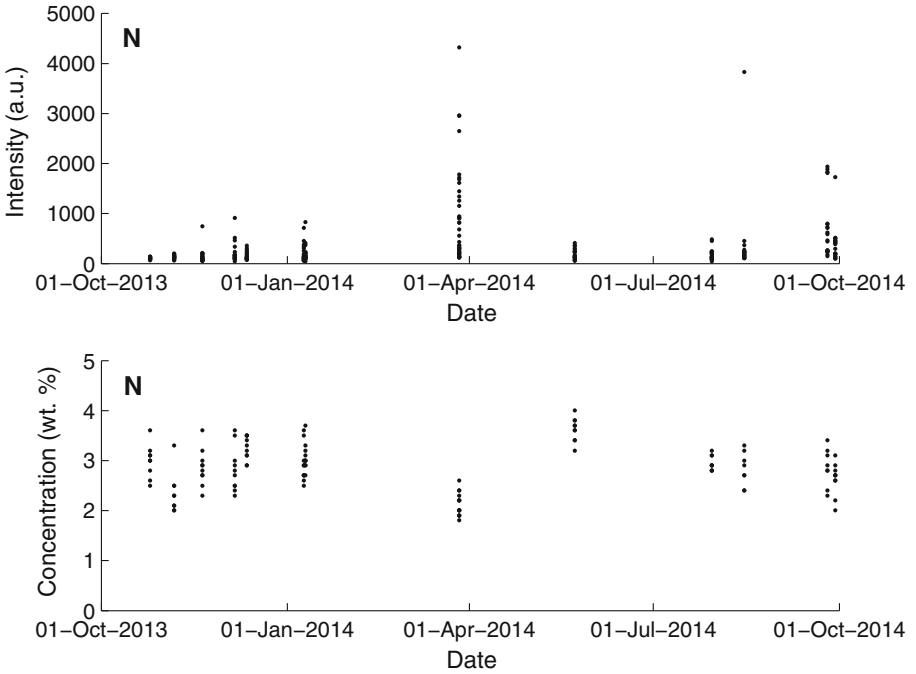

Fig. 4 Moisture effects on the N I 746.83 nm emission line

766.49 nm, K I 769.90 nm, Ca I 422.67 and Na I 589.00 nm respectively. The PLS model built for N may have taken into account the stoichiometric relation between these elements, thus the high VIP scores for K, Ca and Na.

Potassium, sodium and manganese

Besides sodium, the K I 766.49 and K I 769.90 nm lines are the strongest lines in the collected spectra. The cluster of samples with low potassium concentration evident in Fig. 3 is due to pasture harvested during a drought as discussed above. Potassium is the only macro nutrient that gave reasonable results, that is an R^2 greater than 0.9 for pellet samples. The emission lines that received the highest VIP scores for pellets under argon were Na I 589.00 nm, K I 766.49 nm, Na I 589.59 and K I 769.90 nm with scores of 765, 652, 543 and 542. The sodium PLS models performed the best out of all the nutrients studied with a R^2 of 0.93 and a RMSEP of 0.029 wt% for pellets under argon. The large intensities from the sodium D-lines (Na I 589.00 and Na I 589.59 nm) are responsible for the good correlations. The Na I 589.00 nm had the highest VIP score of 842. The strongest manganese line, Mn I 403.08 nm, was weak for fresh pasture, but there are very few spectra that show this emission line. However, the manganese model gives satisfactory results. This is most likely due to the model gaining information from emission lines of other elements that correlate with manganese. This is shown by the Na I 589.00 nm, K I 766.49 nm, K I 769.90 and Na I 589.59 nm receiving the highest VIP scores of 757, 666, 522 and 509 respectively.

Calcium

The Ca II 393.37 and Ca II 396.85 nm lines are the third largest emissions after sodium and potassium. Despite the high intensities from these lines the PLS models do not have high correlations with the actual calcium concentrations. One reason is that the low ionization energy (6.11 eV) for neutral calcium means that there will be emissions from both neutral and ionized calcium. Table 4 lists all the ionization limits of the elements studied in this work. Emission lines from ionized species with ionization energies around 6 eV are commonly observed from LIBS plasmas (Cremers and Radziemski 2013c). The low ionization potential causes large fluctuations in the ratio of neutral to singularly ionized calcium seen between plasmas created on the same sample.

Self-absorption can cause low correlations, but there was no evidence of this in any of the spectra. The resolution of the spectrometer at Ca I 422.727 nm is 0.052 nm and might not be sufficient to show self-absorption. However, this effect usually happens at higher calcium concentrations than the ones discussed in this study (Cremers and Radziemski 2013d).

Potassium and sodium both have ionization potentials lower than calcium. The reason potassium and sodium do not suffer from the same problem as calcium is that the next electron level in the ionized species is so high that it rarely gets populated. This means that the electrons predominantly remain in the ground state, of the ionized species, and very few emissions from ionized potassium or sodium are observed. The emission lines that had a strong influence on the PLS models for pellets under argon were Na I 589.00 nm, K I 766.49 nm, K I 769.90 and Na I 589.59 nm receiving the highest VIP scores of 707, 639, 500 and 490. The calcium lines with the strongest VIP scores were Ca II 393.37 nm, Ca II 396.85 nm, and Ca I 422.67 nm with scores of 308, 213 and 142.

Phosphorus and sulphur

Phosphorus and sulphur do not show any correlations as their strong emission lines are in the ultraviolet region below the measurement range of the spectrometers. The strongest persistent lines are P I 167.97, P I 177.50, S I 142.50, S I 147.40 and S I 180.73 nm. The only phosphorus line that was occasionally observed was a weak P I 253.56 nm line in the

Table 4 Ionization levels of each element's neutral species

Element	Ionization limit (eV)	Next shell (eV)
N	14.53	1.90
P	10.49	1.10
K	4.34	20.15
S	10.36	1.84
Ca	6.11	1.69
Mg	7.65	4.42
Na	5.14	32.85
Fe	7.90	0.23
Mn	7.43	1.17
Zn	9.39	6.01
Cu	7.73	2.72
B	8.30	4.63

The first electron energy level of the singularly ionized element is also listed (Kramida et al. 2017). Each entry is rounded to two decimal places

pellet samples under argon, which had interference with the stronger Fe I 253.56 nm emission line. The VIP score received for this line was 0.067 which means it had very little influence on the model built by PLS. The strongest sulphur line in the region captured by the spectrometers was S I 182.62 nm, which was not visible in any spectra. It had a VIP score of 0.002. The lines that had the strongest VIP scores for both the phosphorus and sulphur were Na I 589.00, K I 766.49, K I 769.90 and Na I 589.59 nm all of which were in the range of 513–796.

Magnesium, copper and iron

The poor calibrations curves for magnesium, copper and iron are due to their weak emission lines. The PLS models are highly influenced by strong lines which is reflected in the VIP scores. The first magnesium line that appears in the VIP scores, for pellets under argon, is 76th with a VIP score of 8.5. The highest VIP score was 755 for a sodium line. The VIPs suggest that sodium, potassium, calcium, argon and hydrogen are more important for the model than the magnesium lines. Copper produces similar results. The Cu I 324.75 nm and Cu I 327.40 nm lines were the strongest copper lines found. The Cu I 324.75 nm line was ranked the 108th variable of importance with a VIP score of 4.9 for pellet samples under argon. Sodium, potassium, calcium and argon displayed the strongest importance in the model, with Na I 589.59 nm having the highest VIP score of 698. The weak VIP scores for copper are evidence for the model's lack of dependence on the copper lines. Calculating the VIPs for the iron model produces no iron lines with a score greater than one. This means the model is not significantly influenced by the iron emissions and is based on secondary correlations with emissions from other elements. The strongest iron line found in the spectra was the Fe II 238.20 nm line. Figure 5 displays a region in the spectra with a few of the strongest iron lines. Each of the 280 spectra for pellets under argon are overlaid on top of each other. These lines are over 100 times smaller than the largest emission lines.

Zinc and boron

Emissions from zinc and boron are not observed consistently on the samples investigated. The strongest zinc line, Zn I 213.86 nm, could only be observed in pellet samples under argon. The strongest boron emission was from B I 249.77 nm which was just above the noise floor and, in some instances, was not observed at all. This produces poor correlations between the models and the actual zinc and boron concentrations. The high R^2 values for both zinc and boron, in pellets sampled under argon, are produced because the lines that influenced the PLS models were Na I 589.00 nm, K I 766.49 nm, K I 769.90 nm and Na I 589.59 nm. The VIP scores for these lines were between 414 and 646. These zinc and boron lines received VIP scores of 0.03 and 0.0009 respectively.

To conclude, the use of an argon purge had mixed results. When used on fresh pasture, there was increased R^2 for all elements except P, better RMSECV for all nutrients except P, Ca and Cu, poorer precision and improved LOD for S, Ca, Mg, Na, Fe, Mn and Zn. An argon purge used on pelletized pasture increased the R^2 for all elements except S, Ca, Mn and B. It reduced the RMSECV and enhanced the precision for N, K, Ca, Mg, Fe, Zn and Cu. It also improved LOD for N, P, Mg, Na, Fe, Zn and Cu. Dried pellets had better R^2 and RMSECV results because there was less between-sample variation caused by the different moisture levels between each fresh sample. The precision for N, P, S, Fe and B were worse in dried pasture. The inability to create high correlating models is due to the shot-to-shot

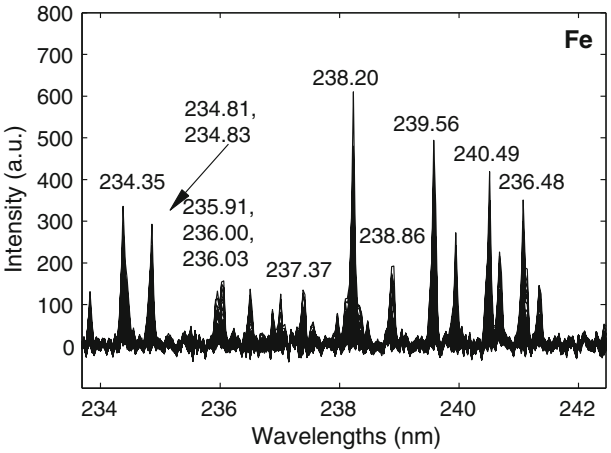

Fig. 5 The strongest iron lines found in the spectral range studied. All spectra are displayed

variation inherent in LIBS. This variation is caused by many factors including sample inhomogeneity, matrix effects, perturbations in experimental parameters, amount of ablated material and the temperature dependence of plasmas (Hahn and Omenetto 2012). The limitation on measuring fresh pasture is the between-sample variation caused by the range of moisture levels existing in pasture which affect emission line intensities.

In field feasibility

Using LIBS to quantitatively measure fresh pasture, under laboratory conditions, had limited success. The nutrient models for fresh pasture were inferior to models created from spectra generated on dried pasture. K, Fe, Mn, Zn and Cu had R^2 values higher than 0.5 with RMSECVs of 0.35, 0.0051, 0.0013, 0.0009 and 0.00011 wt%, respectively. These values are not accurate enough for quantitative measurements but are sufficient to estimate semi-quantitative levels of nutrients. Our laboratory results indicate what might be achievable with an equivalent in-field system although lesser performance should be expected due to greater variability. However, in-field LIBS measurements could be used to identify whether nutrient levels are within a certain range or not. Decisions can then be made in real time as to the type of fertilizer needed in specific areas of a field. The fertilizer application would be sub-optimal but would be an improvement compared to covering an entire field with excess or too little fertilizer.

Implementing an in-field LIBS system to measure herbage would require an autofocus system to mitigate the variability caused by lens-to-sample distance. A successful auto-focus system using the setup in this study was reported by Jull et al. (2017). A similar LIBS unit could then be mounted on agricultural machinery or an agricultural robot to perform measurements and give real-time feedback for tailored fertilizer application. Additional mechanical assemblies would be required to reduce vibration and shock caused from navigating uneven terrain, and issues related to laser safety need to be addressed.

Conclusions

Results indicate that flushing pasture samples with argon while obtaining LIBS spectra has mixed effects. R^2 was increased for every element in fresh pasture except P, RMSECV was reduced for pelletized samples, and precision was reduced for every element in fresh pasture. When comparing fresh and dried pasture, there were reductions in RMSECV for all elements in dried pasture but increases in R^2 for all elements. Results for precision and LOD were mixed. The reason that the dried pellets had better RMSECV results were that there is less between-sample variation caused by the different moisture levels between each fresh sample.

Fresh pasture generates weak spectral emissions at the laser energy used in this study. N, P, Mg, Fe and Cu models all suffer from this problem. The N model also has an interfering contribution from the atmosphere, and the P model has interference from Fe spectra. Zn and B have extremely weak emission lines. Zn lines only appeared under argon, and B lines occasionally did not appear at all. Another confounding issue for Ca and Mg is ionization, where the amount of the element in the plasma is split between neutral and ionized states and the amount of ionization taking place is not consistent between shots. A final issue was that the persistent lines for S only appeared in the ultraviolet range, out of the range of the spectrometers. One way to overcome the problem is to increase the temperature in the plasma. This can be achieved through increasing the power of the laser pulse. Increasing the temperature in the plasma would increase the emission line strength, increase the number of emission lines present in the spectrum and produce full ionization of Ca and Mg, all of which will lead to improvements in actual concentration prediction by calibration models.

Using dried pellets under an argon atmosphere provides the most accurate and precise determination of the elements in pasture. This work showed how accurate LIBS is when used on fresh herbage and what performance could be expected in-field. Different laser parameters, such as wavelength, pulse energy and pulse duration, may increase accuracy.

This is the first time LIBS has been used on fresh pasture samples. Successful calibration curves on pasture pellets, all having an R^2 greater than 0.90, were made for K, Na and Mn. The laboratory results suggest that semi quantitative analyses can be made in-field on fresh pasture to create estimates of nutrient levels. The estimates could then be used to influence fertilizer application.

Acknowledgements We would like to acknowledge and offer continuing respect and admiration to deceased colleague Dr. Sadhana Talele, who was not able to see this work completed. Financial assistance from the New Zealand Ministry of Business, Innovation and Employment under contract C11X1209 is gratefully acknowledged.

References

Allegrini, F., & Olivieri, A. C. (2014). IUPAC-consistent approach to the limit of detection in partial least-squares calibration. *Analytical Chemistry, 86*(15), 7858–7866. https://doi.org/10.1021/ac501786u.

ASTM E1655-05. (2012). *Standard practices for infrared multivariate quantitative analysis*. West Conshohocken, PA, USA: ASTM International.

Barker, A. V., & Pilbeam, D. J. (2006). *Handbook of plant nutrition* (1st ed.). Boca Raton, FL, USA: CRC Press/Taylor & Francis.

Barnett, W. B., Fassel, V. A., & Kniseley, R. N. (1968). Theoretical principles of internal standardization in analytical emission spectroscopy. *Spectrochimica Acta, Part B: Atomic Spectroscopy, 23*(10), 643–664.

Boqué, R., & Rius, F. X. (1996). Multivariate detection limits estimators. *Chemometrics and Intelligent Laboratory Systems, 32*(1), 11–23. https://doi.org/10.1016/0169-7439(95)00049-6.

Boyain-Goitia, A. R., Beddows, D. C. S., Griffiths, B. C., & Telle, H. H. (2003). Single-pollen analysis by laser-induced breakdown spectroscopy and Raman microscopy. *Applied Optics, 42*(30), 6119–6132.

Braga, J. W. B., Trevizan, L. C., Nunes, L. C., Rufini, I. A., Santos, D., Jr., & Krug, F. J. (2010). Comparison of univariate and multivariate calibration for the determination of micronutrients in pellets of plant materials by laser induced breakdown spectrometry. *Spectrochimica Acta—Part B: Atomic Spectroscopy, 65*(1), 66–74. https://doi.org/10.1016/j.sab.2009.11.007.

Chauhan, D. K., Tripathi, D. K., Rai, N. K., & Rai, A. K. (2011). Detection of biogenic silica in leaf blade, leaf sheath, and stem of bermuda grass (*Cynodon dactylon*) using LIBS and phytolith analysis. *Food Biophysics, 6*(3), 416–423. https://doi.org/10.1007/s11483-011-9219-y.

Chong, I. G., & Jun, C. H. (2005). Performance of some variable selection methods when multicollinearity is present. *Chemometrics and Intelligent Laboratory Systems, 78*(1), 103–112. https://doi.org/10.1016/j.chemolab.2004.12.011.

Cremers, D., & Radziemski, L. (2013a). Introduction. In *Handbook of laser-induced breakdown spectroscopy* (2nd ed., p. 3). West Sussex, UK: Wiley.

Cremers, D., & Radziemski, L. (2013b). Basics of the LIBS plasma. In *Handbook of laser-induced breakdown spectroscopy* (2nd ed., pp. 48–58). West Sussex, UK: Wiley.

Cremers, D., & Radziemski, L. (2013c). Qualitative LIBS analysis. *Handbook of laser-induced breakdown spectroscopy* (pp. 151–183). West Sussex, UK: Wiley.

Cremers, D., & Radziemski, L. (2013d). LIBS analytical figures of merit and calibration. In *Handbook of Laser-Induced Breakdown Spectroscopy* (2nd ed., pp. 131–140). West Sussex, UK: Wiley.

Devey, K., Mucalo, M., Rajendram, G., & Lane, J. (2015). Pasture vegetation elemental analysis by laser-induced breakdown spectroscopy. *Communications in Soil Science and Plant Analysis, 46,* 72–80. https://doi.org/10.1080/00103624.2014.988578.

Fink, H., Panne, U., & Niessner, R. (2002). Process analysis of recycled thermoplasts from consumer electronics by laser-induced plasma spectroscopy. *Analytical Chemistry, 74*(17), 4334–4342. https://doi.org/10.1021/ac025650v.

Gorham, J. (2006). Sodium. In A. V. Barker & D. J. Pilbeam (Eds.), *Handbook of plant nutrition* (1st ed., pp. 573–575). Boca Raton, FL, USA: CRC Press/Taylor & Francis.

Hahn, D. W., & Omenetto, N. (2012). Laser-induced breakdown spectroscopy (LIBS), part II: Review of instrumental and methodological approaches to material analysis and applications to different fields. *Applied Spectroscopy, 66*(4), 347–419. https://doi.org/10.1366/11-06574.

Jull, H., Ewart, P., Künnemeyer, R., & Schaare, P. (2017). Selective surface sintering using a laser-induced breakdown spectroscopy system. *Journal of Spectroscopy, 2017,* 1–11. https://doi.org/10.1155/2017/1478541.

Jull, H., Künnemeyer, R., Talele, S., Schaare, P., & Seelye, M. (2015). Laser-induced breakdown spectroscopy analysis of sodium in pelletised pasture samples. In D. Bailey, S. Demidenko, & G. S. Gupta (Eds.), *6th International conference on automation, robotics and applications, ICARA 2015* (pp. 262–268). Danvers, MA, USA: Institute of Electrical and Electronics Engineers Inc. https://doi.org/10.1109/icara.2015.7081157.

Kramida, A., Yu. Ralchenko, Reader, J., & NIST ASD Team. (2017). NIST Atomic Spectra Database (ver. 5.2). Retrieved January 3, 2018, from http://physics.nist.gov/asd.

Lazic, V., Rauschenbach, I., Jovicevic, S., Jessberger, E. K., Fantoni, R., & Di Fino, M. (2007). Laser induced breakdown spectroscopy of soils, rocks and ice at subzero temperatures in simulated Martian conditions. *Spectrochimica Acta—Part B: Atomic Spectroscopy, 62*(12), 1546–1556. https://doi.org/10.1016/j.sab.2007.10.006.

Martin, M. Z., Stewart, A. J., Gwinn, K. D., & Waller, J. C. (2010). Laser-induced breakdown spectroscopy used to detect endophyte-mediated accumulation of metals by tall fescue. *Applied Optics, 49*(13), C161–C167.

Mehmood, T., Martens, H., Sæbø, S., Warringer, J., & Snipen, L. (2011). A partial least squares based algorithm for parsimonious variable selection. *Algorithms for Molecular Biology, 6*(1), 1–12. https://doi.org/10.1186/1748-7188-6-27.

Nunes, L. C., Batista Braga, J. W., Trevizan, L. C., Florêncio De Souza, P., Arantes De Carvalho, G. G., Júnior, D. S., et al. (2010). Optimization and validation of a LIBS method for the determination of macro and micronutrients in sugar cane leaves. *Journal of Analytical Atomic Spectrometry, 25*(9), 1453–1460.

Ortiz, M. C., Sarabia, L. A., Herrero, A., Sánchez, M. S., Sanz, M. B., Rueda, M. E., et al. (2003). Capability of detection of an analytical method evaluating false positive and false negative (ISO 11843) with

partial least squares. *Chemometrics and Intelligent Laboratory Systems, 69*(1), 21–33. https://doi.org/10.1016/S0169-7439(03)00110-2.

Rai, P. K., Jaiswal, D., Rai, N. K., Pandhija, S., Rai, A. K., & Watal, G. (2009). Role of glycemic elements of *Cynodon dactylon* and *Musa paradisiaca* in diabetes management. *Lasers in Medical Science, 24*(5), 761–768.

Rauschenbach, I., Lazic, V., Pavlov, S. G., Hübers, H. W., & Jessberger, E. K. (2008). Laser induced breakdown spectroscopy on soils and rocks: Influence of the sample temperature, moisture and roughness. *Spectrochimica Acta—Part B: Atomic Spectroscopy, 63*(10), 1205–1215. https://doi.org/10.1016/j.sab.2008.08.006.

Thakur, S. N. (2007). Atomic emission spectroscopy. In J. P. Singh & S. N. Thakur (Eds.), *Laser-induced breakdown spectroscopy* (pp. 29–30). Oxford, UK: Elsevier.

van Maarschalkerweerd, M., & Husted, S. (2015). Recent developments in fast spectroscopy for plant mineral analysis. *Frontiers in Plant Science, 6,* 169. https://doi.org/10.3389/fpls.2015.00169.

Wold, S., Johansson, E., & Cocchi, M. (1993). PLS—partial least-squares projections to latent structures. In H. Kubinyi (Ed.), *3D QSAR in drug design: Theory, methods and applications* (pp. 523–550). Leiden, The Netherlands: ESCOM.